

Taking snapshots of a moving electron wave packet in molecules using photoelectron holography in strong-field tunneling ionization

Mingrui He(何明睿), Yang Fan(樊洋), Yueming Zhou(周月明), and Peixiang Lu(陆培祥)
Citation: Chin. Phys. B, 2021, 30 (**12**): 123202. DOI: 10.1088/1674-1056/abf7a7
Journal homepage: http://cpb.iphy.ac.cn; http://iopscience.iop.org/cpb

What follows is a list of articles you may be interested in

HeTDSE: A GPU based program to solve the full-dimensional time-dependent Schrödinger equation for two-electron helium subjected to strong laser fields

Xi Zhao(赵曦), Gangtai Zhang(张刚台), Tingting Bai(白婷婷), Jun Wang(王俊), and Wei-Wei Yu(于伟威)
Chin. Phys. B, 2021, 30 (**7**): 073201. DOI: 10.1088/1674-1056/abe1a4

High-precision three-dimensional Rydberg atom localization in a four-level atomic system

Hengfei Zhang(张恒飞), Jinpeng Yuan(元晋鹏), Lirong Wang(汪丽蓉), Liantuan Xiao(肖连团), and Suo-tang Jia(贾锁堂)
Chin. Phys. B, 2021, 30 (**5**): 053202. DOI: 10.1088/1674-1056/abd46f

Imprint of transient electron localization in H_2^+ using circularly-polarized laser pulse

Jianghua Luo(罗江华), Jun Li(李军), and Huafeng Zhang(张华峰)
Chin. Phys. B, 2020, 29 (**12**): 123201. DOI: 10.1088/1674-1056/abbbe1

Bohmian trajectory perspective on strong field atomic processes

Xuan-Yang Lai(赖炫扬), Xiao-Jun Liu(柳晓军)
Chin. Phys. B, 2020, 29 (**1**): 013205. DOI: 10.1088/1674-1056/ab5c0f

Backward rescattered photoelectron holography in strong-field ionization

Fujun Chen(陈富军), Ruxian Yao(姚汝贤), Jianghua Luo(罗江华), Changqing Wang(王长清)
Chin. Phys. B, 2018, 27 (**10**): 103202. DOI: 10.1088/1674-1056/27/10/103202

Taking snapshots of a moving electron wave packet in molecules using photoelectron holography in strong-field tunneling ionization*

Mingrui He(何明睿)[1,†], Yang Fan(樊洋)[1], Yueming Zhou(周月明)[2], and Peixiang Lu(陆培祥)[2]

[1] Department of Basic Courses, Naval University of Engineering, Wuhan 430033, China

[2] School of Physics and Wuhan National Laboratory for Optoelectronics, Huazhong University of Science and Technology, Wuhan 430074, China

(Received 9 February 2021; revised manuscript received 5 April 2021; accepted manuscript online 14 April 2021)

Coherent superposition of electronic states induces attosecond electron motion in molecules. We theoretically investigate the strong-field ionization of this superposition state by numerically solving the time-dependent Schrödinger equation. In the obtained photoelectron momentum distribution, an intriguing bifurcation structure appears in the strong-field holographic interference pattern. We demonstrate that this bifurcation structure directly provides complete information about the status of the transient wave function of the superposition state: the horizontal location of the bifurcation in the momentum distribution reveals the relative phase of the involved components of the superposition state and the vertical position indicates the relative coefficient. Thus, this bifurcation structure takes a snapshot of the transient electron wave packet of the superposition state and provides an intuitive way to monitor electron motion in molecules.

Keywords: strong-field ionization, photoelectron holography, charge migration

PACS: 32.80.Rm, 42.65.Re, 32.80.Fb **DOI:** 10.1088/1674-1056/abf7a7

1. Introduction

Exploring attosecond electronic dynamics in atoms and molecules is one of the most challenging areas in the modern attosecond science.[1] Previous studies have demonstrated that ultrafast electronic dynamics can be induced by strong-field excitation and ionization in virtually all polyatomic molecules.[2–4] The natural time scale of the valence electron dynamics ranges from a few femtoseconds to hundreds of attosenconds.[2,5] Therefore, attosecond temporal resolution is required to achieve the real-time observation. In the past decades, the rapidly developing attosecond techniques open up the way to access the electron motion on their intrinsic time scales,[6–8] inspiring widespread interests on monitoring the ultrafast electronic dynamics.[9] Previously proposed techniques for observing coherent electronic dynamics include high-order harmonic spectroscopy,[10–14] attosecond transient absorption,[15,16] ultrafast streaking[17] and electron wave packet (EWP) interferometric technique,[18–20] etc. Moreover, both x-ray scattering[21] and attosecond electron scattering[22] are also proposed as promising methods to monitor instantaneous electronic density distribution. In the area of strong-field ionization, significant progress on investigating the electronic dynamical information encoded in the photoelectron momentum spectra has been made.[23–27] With these methods, one can access coherent imaging of the attosecond electron motion and realize the control of the chemical and biological reaction process in a further step.

Complementary to those measurements, the rescattering based strong-field photoelectron holography (SFPH) is expected to be an efficient method to image the attosecond valence electron motion.[28–30] Photoelectron holographic structure in the photoelectron momentum distribution (PEMD) results from the interference between the electrons that recollide with the parent ion and electrons that reach the detector directly after tunneling ionization.[31] The rescattering process naturally provides access to both the structural information and the electronic dynamics of the atoms and molecules, and thus makes SFPH a practical photoelectron spectroscopy.[32–34] In our previous works, we extracted the inherent structural information, the phase of the scattering amplitude, from the holographic interference.[35,36] Very recently, we have demonstrated the real-time and *in-situ* observation of the ultrafast charge migration in molecules with attosecond temporal resolution using SFPH.[29] In that scheme, the dynamical information of the electron is retrieved from the phase of the holographic fringes, where especially high momentum resolution is necessary, and this phase extraction process requires a sophisticated procedure.

In this study, we propose a more direct method to take snapshots of the transient valence EWP with the concept of SFPH that avoids any extraction procedure. We investigate the strong-field tunneling ionization of the superposition state of H_2^+ by numerically solving the time-dependent Schrödinger equation (TDSE). For the non-stationary superposition state, an unexpected bifurcation structure appears in the holographic pattern in the obtained PEMD. We demonstrate that this bifur-

*Project supported by the National Natural Science Foundation of China (Grant Nos. 11874163, 11604108, and 11604388), the Program for HUST Academic Frontier Youth Team, and the Fundamental Research Funds for the Central Universities, China (HUST No. 2017KFXKJC002).

†Corresponding author. E-mail: hmr_emma@163.com

© 2021 Chinese Physical Society and IOP Publishing Ltd

cation structure encodes complete information of the transient electron wave function. The location of this bifurcation in the PEMD reveals the transient relative phase and the relative coefficient of the EWP. With this information, the transient EWP of the superposition state is directly visualized. Further, by investigating the superposition states with different relative coefficients ionized by the laser fields with different parameters, the accuracy and robustness of our method are verified. Our work provides a direct approach to visualize the valence electron motion with the concept of SFPH. Note that this bifurcation structure should be more easily observed in experiments. It will encourage further experimental attempt on exploring ultrafast electronic dynamics in molecules.

2. Numerical methods

In our investigation, we employ the prototypical H_2^+ molecular ion with fixed bond length as a sample molecule, which is widely applied in the theoretical investigation of the electron motion of the surperposition state.[26,27] The H_2^+ molecular ion is prepared in the coherent superposition of two electronic states

$$\psi(\boldsymbol{r},t) = c_1\psi_1(\boldsymbol{r})\,\mathrm{e}^{-\mathrm{i}E_1 t} + c_2\psi_2(\boldsymbol{r})\,\mathrm{e}^{-\mathrm{i}(E_2 t+\theta_0)}, \quad (1)$$

where $\psi_1(\boldsymbol{r})$ is the ground state ($1s\sigma_g$) and $\psi_2(\boldsymbol{r})$ is the first excited state ($2p\sigma_u$); $c_{1,2}$ are expansion coefficients of the two states ($c_1^2 + c_2^2 = 1$); and θ_0 is the initial relative phase that is adjustable by changing the pump-probe delay in experiments.

To investigate the ionization of this superposition state in the few-cycle laser field, we numerically solve the two-dimensional TDSE and calculate the PEMD.[37] In the length gauge, the Hamiltonian $\mathcal{H}(\boldsymbol{r},t)$ of the system is given by (atomic units are used unless stated otherwise)

$$\mathcal{H}(\boldsymbol{r},t) = -\frac{1}{2}\nabla^2 + V(\boldsymbol{r}) + \boldsymbol{r}\cdot\boldsymbol{E}(t). \quad (2)$$

Here $\boldsymbol{r} = (x,y)$ in the two-dimensional space. We adopt a two-center soft-core molecular potential $V(x,y) = -1/\sqrt{x^2+(y-R/2)^2+\eta} - 1/\sqrt{x^2+(y+R/2)^2+\eta}$ to mimic H_2^+, which is aligned along y-axis with internuclear separation $R = 4$ a.u. The soft-core parameter η is set to be 0.715 to reproduce the energy of the ground state $E_1 = -0.7963$ a.u. and that of the first excited state $E_2 = -0.6551$ a.u. Thus, the oscillation period of this superposition state is $\mathrm{T} = 2\pi/\Delta E = 44.5$ a.u. During this ultrashort time interval, the nuclear motion could be neglected. We mention that the moving of the nuclei will deteriorate the coherence of the superposition state to some degree in a long time scale,[38,39] and thus it should be taken into consideration for the long-cycle laser pulse. For the few-cycle laser pulse, we apply the fixed nuclei approximation in our calculation. $\boldsymbol{E}(t)$ represents the electric field of the few-cycle laser pulse which is linearly polarized along x-axis (perpendicular to the aligned molecule). This electric field is defined as

$$\boldsymbol{E}(t) = E_0\,\mathrm{e}^{-2\ln 2(t/\tau)^2}\cos(\omega t)\boldsymbol{x}. \quad (3)$$

Here E_0 is the peak intensity, τ is the pulse duration, ω is the angular frequency of the laser pulse; $\boldsymbol{x}$ is the unit vector along x direction. This electric field ensures that the vector potential is zero at the beginning and the end of the laser pulse.

The split-operator spectral method on a Cartesian grid is used to solve the TDSE.[37] In our simulation, the time step of propagation is $\Delta t = 0.1$ a.u. At the end of the laser pulse, the wave function is further propagated for additional 1000 a.u. to ensure that all the ionized components are collected. The Cartesian grid ranges from -400 a.u. to 400 a.u. for both directions with $\Delta x = \Delta y = 0.2$ a.u. Convergence is checked with respect to the spatial and temporal grid densities and sizes.

3. Formation of the bifurcation in the photoelectron momentum distribution

We use a 2000 nm pulse with the intensity of 3.0×10^{14} W/cm^2 and full width at half maximum (FWHM) of 11.5 fs to ionize H_2^+. The PEMDs for the tunneling ionization of the ground state and the superposition state (with $c_1 : c_2 = 2$ and $\theta_0 = 0$) are presented in Figs. 1(a) and 1(b), respectively. Several kinds of interference patterns are entangled with each other in the PEMD. The ring-like pattern visible in the low energy part is the familiar above-threshold ionization (ATI) structure,[40] which results from the interference of the EWPs tunneling ionized at different laser cycles. The nearly vertical fine fringes are the intracycle interference fringes of electrons liberated at adjacent half cycles, which are usually interpreted as the time-domain double-slit interference fringes.[40–42] These stripes are hardly observed in experiments because their positions are very sensitive to the laser field intensities, and thus are averaged out in the integrated signal from the laser focal volume. The most pronounced nearly horizontal fringes are the near-forward SFPH we will focus on.[31] For the PEMD of the ground state, this type of interference is exactly symmetric about $p_y = 0$, while for the superposition state, it is obviously asymmetric about $p_y = 0$. In our previous study, we proposed a sophisticated procedure to extract the electronic dynamics of the superposition state from these asymmetric SFPH patterns.[29] Intriguingly, in Fig. 1(b), a clear bifurcation structure appears in the PEMD (at $p_x = -2.27$ a.u., $p_y = 0.20$ a.u.), where the first- and second-order interference maxima merge into a single fringe, as indicated by the white square. This structure is absent in the PEMD of the ground state. In the following, we will show that this structure is a consequence of the electron motion of the non-stationary state and it provides snapshots of the transient EWP of this state.

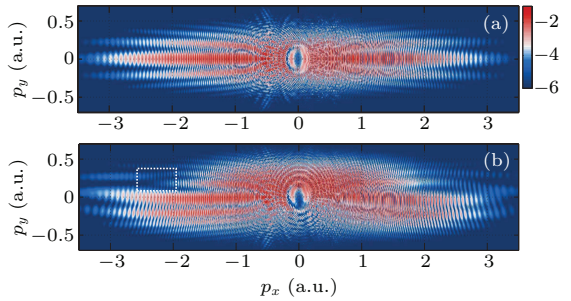


Fig. 1. (a) Photoelectron momentum distribution (PEMD) for the tunneling ionization of the ground state of H_2^+ by the few-cycle laser pulse. The wavelength of this laser pulse is 2000 nm and the intensity is 3.0×10^{14} W/cm^2. The pulse duration (FWHM) is 11.5 fs. (b) The same as (a), but for the superposition state of H_2^+, which is composed of the ground state $1s\sigma_g$ and the first excited state $2p\sigma_u$ with expansion coefficients $c_1=\sqrt{4/5}$ and $c_2=\sqrt{1/5}$. The white square indicates the bifurcation structure.

As demonstrated in our previous works,[29,35] the holographic structure originates from the interference between the EWPs that reach the detector with and without the near-forward rescattering by the parent ion,

$$|I_d+I_r|^2=|I_d|^2+|I_r|^2+2|I_d||I_r|\cos(\Delta\varphi), \tag{4}$$

where I_d and I_r are the direct and rescattering parts of the ionization amplitude, respectively.[43] $\Delta\varphi$ is the interference phase in the form[29,35]

$$\Delta\varphi=\frac{1}{2}p_y^2(t_r-t_i)+\alpha+[\phi(0;t_i)-\phi(p_y;t_i)]. \tag{5}$$

Here p_y is the transverse momentum, $t_{i,r}$ are the instants of the ionization and recollision, respectively. The first term on the right-hand side of Eq. (5) has a classical origin and has been discussed in Refs. [31,44]. The second term α is the phase of the scattering amplitude, which is first revealed in Ref. [35]. The third term is related to the electronic dynamics of the nonstationary state.[29] Here, $\phi(p_y;t_i)$ and $\phi(0;t_i)$ are the phases of transverse momentum distribution amplitudes (TMDAs) for the direct and rescattering electrons at the instant of tunneling, respectively. Note that for the rescattering electron, the initial transverse momentum at tunneling should be zero, and for the direct electron, the final transverse momentum equals the initial value.[29] The TMDA of the ground state possesses a global phase, and thus the third term $\phi(0;t_i)-\phi(p_y;t_i)=0$ disappears in Eq. (5). For the superposition state, as the electron wave function evolves, the TMDA has nontrivial phase structure, so that the third term in Eq. (5) contains valuable information about the electron motion. In this case, the TMDA has the form

$$A(p_y;t)=c_1A_1(p_y)+c_2A_2(p_y)\,e^{-i\theta(t)}, \tag{6}$$

where $\theta(t)=\Delta Et+\theta_0$ and $A_{1,2}$ represent TMDAs of $1s\sigma_g$ and $2p\sigma_u$ states, respectively. To explain the formation of the bifurcation in Fig. 1(b), we calculate the TMDAs with the same laser parameters as those used in Fig. 1. The moduli of $A_{1,2}$ are presented by the solid colored curves in Fig. 2(c). For $1s\sigma_g$ state, the modulus of the TMDA has a Gaussian-like form. For the $2p\sigma_u$ state, the modulus of the TMDA has a node at $p_y=0$. The phases of $A_{1,2}$ are also shown in Fig. 2(c) by the dashed-dotted curves. For $A_1(p_y)$, it is always zero, and for $A_2(p_y)$, there is a jump from $\pi/2$ to $-\pi/2$ at $p_y=0$. The phase of the TMDA of the superposition state can be expressed as

$$\begin{aligned}\phi(p_y;t)&=\arg[A(p_y;t)]\\&=\arg\left\{|c_1A_1(p_y)|+|c_2A_2(p_y)|\,e^{-i[\frac{\pi}{2}\mathrm{sgn}(p_y)+\theta(t)]}\right\},\end{aligned} \tag{7}$$

where sgn is the sign function. In Figs. 2(d) and 2(e), we display $\phi(p_y;t)$ at different instants. It is clearly shown that these phases are smooth functions of p_y except the instants of $t=0.25$ T and 0.75 T, where there are abrupt jumps. Because of the phase jump in the TMDA, the holographic interference phase [as expressed by Eq. (5)] jumps accordingly. Thus, the bifurcation structure appears in the holographic pattern.

According to Eq. (7), the phase jump in the phase of the TMDA should appear at $|c_1A_1(p_y)|=|c_2A_2(p_y)|$ and $\frac{\pi}{2}\mathrm{sgn}(p_y)+\theta(t)=(2n+1)\pi$. For example, for the superposition state of H_2^+ with $c_1:c_2=2$, the phase jump of $\phi(p_y;t)$ should occur at $p_y=0.22$ a.u. (-0.22 a.u.) and $\theta(t)=\pi/2$ ($3\pi/2$), as shown in Fig. 2(d) [Fig. 2(e)]. In Figs. 2(f)–2(i), we plot the moduli and phases of the electron wave functions of the superposition states with $\theta(t)=\pi/2$ and $3\pi/2$, respectively. For these relative phases, the electron is delocalized in the molecule. The above analysis indicates that when the bifurcation structure appears in the PMED, the relative coefficient and phase of the involved states can be deduced. Consequently, the instantaneous electron wave function of the superposition state is obtained. In Fig. 1(b), the bifurcation structure is located at $p_x=2.27$ a.u. and $p_y=0.20$ a.u. Based on our above explanation, at the instant of tunneling ionization for $p_x-2.27$ a.u., the relative phase should be $\theta(t)=2n\pi+\pi/2$. The transverse location of $p_y=0.20$ a.u., which is very close to the predicated location 0.22 a.u. for $c_1:c_2=2$, indicating that the relative coefficient $c_1:c_2$ can be accurately retrieved.

Figure 3 presents the reconstructed electron wave function of the superposition state with the relative phase and coefficients deduced from the location of the bifurcation structure in Fig. 1(b). First, from the longitudinal location p_x, we retrieve the instant of tunneling ionization $t_i=25.98$ a.u. (as indicated by the orange asterisk in Fig. 3(a)) by applying the classical relation $p_x=-\frac{1}{2}\int_{t_i}^{\infty}E(t)\,dt$. At this instant, the relative phase of the superposition state should be $2n\pi+\pi/2$. Then, we substitute the transverse location $p_y=0.20$ a.u. into the equality $|c_1A_1(p_y)|=|c_2A_2(p_y)|$. The deduced relative coefficient $c_1:c_2$ is 1.76, which is close to that used in our calculation ($c_1:c_2=2$). With this information, we reconstruct the electron wave function as shown in Figs. 3(b) (modulus) and 3(c) (phase). Thus, the snapshot of the transient EWP of the superposition state is obtained successfully. In what follows, we will exam the accuracy and robustness of our method.

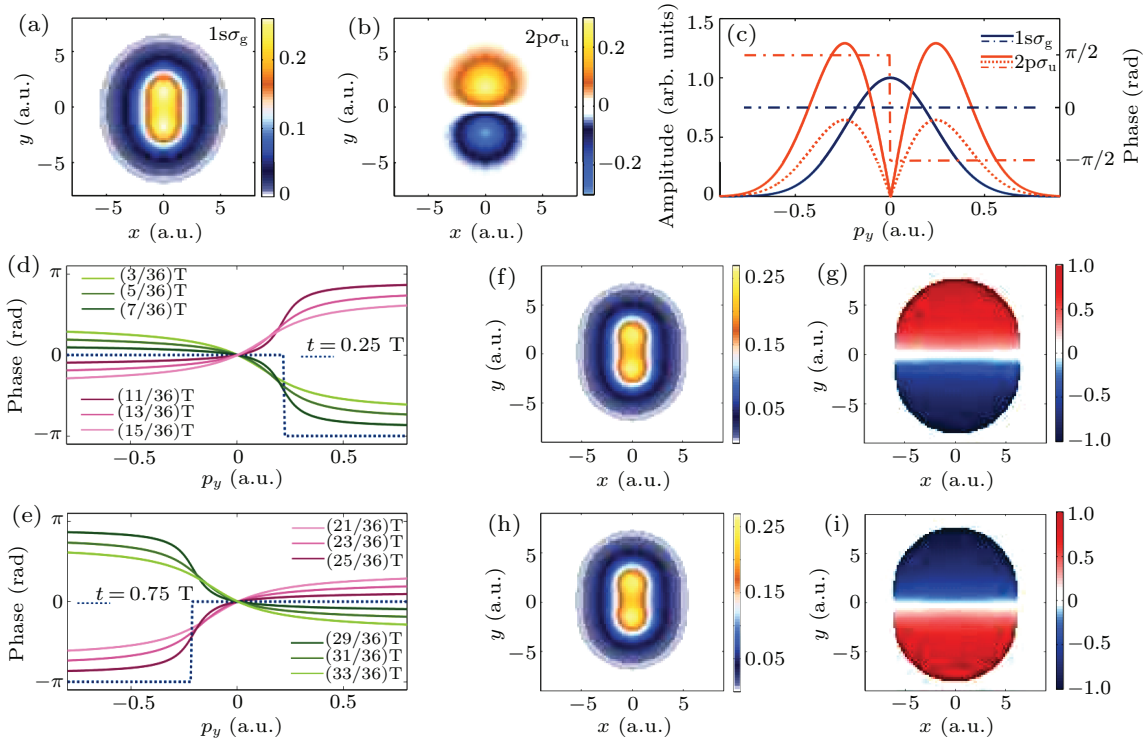


Fig. 2. (a) and (b) The electron wave functions of the ground state $1s\sigma_g$ and the first excited state $2p\sigma_u$ of H_2^+ in coordinate space, respectively. (c) The transverse momentum distribution amplitudes (TMDAs) $A_{1,2}$ of $1s\sigma_g$ state (blue curves) and $2p\sigma_u$ state (orange curves). The moduli of the amplitudes are shown as the solid curves, and the phases are shown as dash-dotted lines. The dotted orange curve represents the quantity $|A_2(p_y)|/2$. The laser parameters are the same as Fig. 1. (d) and (e) The phases of TMDAs of the superposition state with $c_1 : c_2 = 2$ at different instants around $t = 0.25$ T and $t = 0.75$ T. (f) and (g) The modulus and phase of the EWP of the superposition state at the instant of $t = 0.25$ T. (h) and (i) The same as (f) and (g) but at the instant of $t = 0.75$ T.

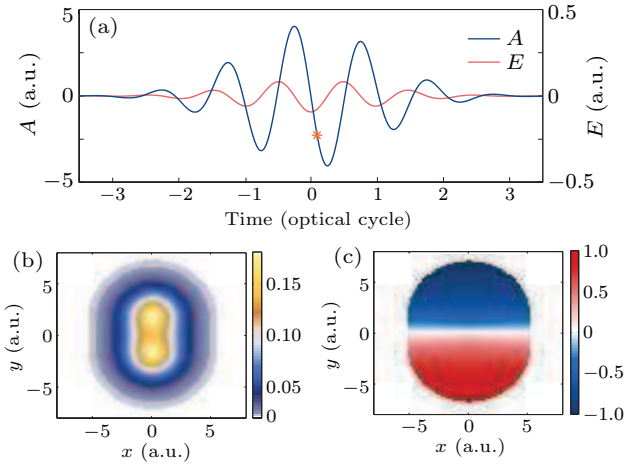


Fig. 3. (a) The electric field (red curve) and the vector potential (blue curve) of the few-cycle laser pulse used in Fig. 1. The orange asterisk indicates the tunneling ionization time corresponding to the longitudinal momentum of the bifurcation structure in Fig. 1(a). (b) and (c) The reconstructed modulus and phase of the electron wave function of the superposition state at the instant indicated by the asterisk in (a), respectively.

We investigate the ionization of the superposition state of H_2^+ with the initial phase $\theta_0 = 0.5\pi$ and relative coefficient $c_1 : c_2$ ranges from 2 to 6 in the 2000 nm laser field. Here the intensity of the laser field is 3.0×10^{14} W/cm^2 and the duration (FWHM) is 6.9 fs. As explained above, the transverse location p_y of the bifurcation structure should satisfy the equation $|c_1 A_1(p_y)| = |c_2 A_2(p_y)|$, and thus it changes with $c_1 : c_2$. As presented in Fig. 4(c), p_y of the bifurcation structure for different $c_1 : c_2$ is indicated by the crossing of the solid blue curve and the corresponding dotted curve. Here two sets of cross points appear. The positive (negative) set of p_y corresponds to the relative phase $\theta(t) = 2n\pi + \pi/2$ ($2n\pi + 3\pi/2$). In the obtained PEMDs, clear bifurcation structures appear with positive p_y. Two examples of the bifurcation structures are shown in Figs. 4(a) and 4(b), indicated by the white squares in the PEMDs for $c_1 : c_2 = 2$ and 3, respectively. The longitudinal locations p_x of them are close to each other (2.08 a.u. and 2.03 a.u. in Figs. 4(a) and 4(b), respectively). The corresponding ionization time for $p_x = 2.03$ a.u. is $t = 23.5$ a.u. At this instant, the relative phase of the superposition state should be $2n\pi + \pi/2$. The transverse locations p_y of the bifurcation structures change with the relative coefficients, as presented by the red circles in Fig. 4(d). For comparison, we present the precise solution (positive set) of the equality $|c_1 A_1(p_y)| = |c_2 A_2(p_y)|$ as a function of $c_1 : c_2$ by the solid blue curve. One can find that the agreement between the red circles and the blue curve is prominent for large p_y, while the red circle deviates from the blue curve slightly at small p_y. This is because the influence of the coulomb potential is more remarkable for the electron with small transverse momentum. These results demonstrate that the transverse location of the bifurcation structure is sensitive to the relative coefficient, and thus it provides accurate information about the EWP of the non-stationary state.

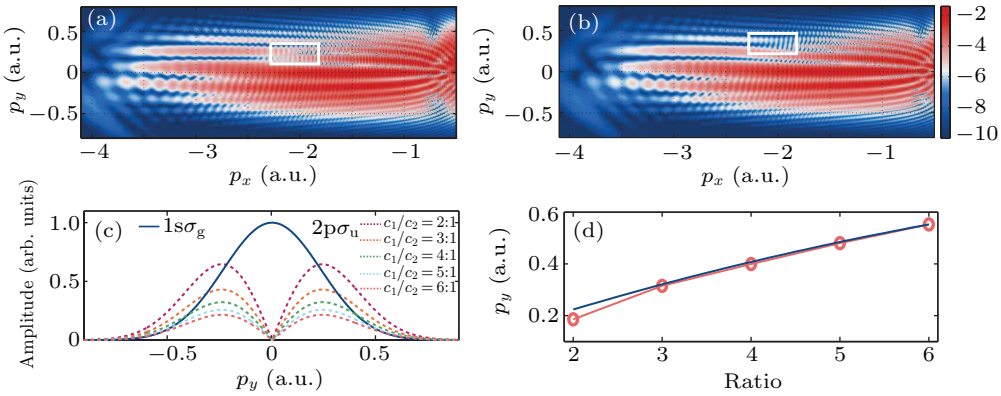


Fig. 4. (a) The PEMD of the superposition state with the relative coefficient $c_1 : c_2 = 2$ and the initial relative phase $\theta_0 = 0.5\pi$. (b) The same as (a) but for $c_1 : c_2 = 3$. (c) The solid curve represents the modulus of the TMDA of $1s\sigma_g$ state ($|A_1|$). The colored dotted curves indicate the quantity $c_2|A_2(p_y)|/c_1$ with five different relative coefficients $c_1 : c_2$. (d) The red circles indicate the transverse momenta of the bifurcations extracted from the PEMDs for the superposition state with five different relative coefficients as same as (c). The blue curve present the precise solution (positive set) of the equality $c_1|A_1(p_y)| = c_2|A_2(p_y)|$ as a function of the ratio $c_1 : c_2$ for comparison. The FWHM of the laser pulse is about 6.9 fs and the intensity of the laser pulse is 3.0×10^{14} W/cm^2.

4. Conclusion

In summary, we have proposed a method based on SFPH to take snapshots of the EWP of the superposition state. For the strong-field tunneling ionization of the coherent superposition state of H_2^+, an interesting bifurcation structure appears in the PEMD, which encodes complete information about the transient electron wave function. The longitudinal location of this structure indicates the transient relative phase between the components of the superposition state, and the transverse location reveals the relative coefficient. With this information, we are able to obtain the instantaneous electron wave function of the superposition state. Then we apply our method to investigate the coherent superposition states with different relative coefficients. The transient EWPs of these states are obtained by investigating the bifurcation structure. This result demonstrates that our method is efficient to visualize the ultrafast electron motion. Our work provides a feasible approach to monitor the electron motion in more complicated molecules.

References

[1] Lépine F, Ivanov M Y and Vrakking M J J 2014 *Nat. Photon.* **8** 195

[2] Breidbach J and Cederbaum L S 2005 *Phys. Rev. Lett.* **94** 033901

[3] Grønager M and Henriksen N E 1997 *Chem. Phys. Lett.* **278** 166

[4] Bandrauk A D, Chelkowski S and Nguyen H S 2004 *Int. J. Quantum Chem.* **100** 834

[5] Remacle F and Levine R D 2006 *Proc. Natl. Acad. Sci.* **103** 6793

[6] López-Martens R, Varjú K, Johnsson P, Mauritsson J, Mairesse Y, Salières P, Gaarde M B, Schafer K J, Persson A, Svanberg S, Wahlström C and L'Huillier A 2005 *Phys. Rev. Lett.* **94** 033001

[7] Gaumnitz T, Jain A, Pertot Y, Huppert M, Jordan I, Ardana-Lamas F and Wörner H J 2017 *Opt. Express* **25** 27506

[8] Yan J, Xie W, Li M, Liu K, Luo S, Cao C, Guo K, Cao W, Lan P, Zhang Q, Zhou Y and Lu P 2020 *Phys. Rev. A* **102** 013117

[9] Xu S, Zhang Q, Ran C, Huang X, Cao W and Lu P 2021 *Chin. Phys. B* **30** 013202

[10] Niikura H, Villeneuve D M and Corkum P B 2005 *Phys. Rev. Lett.* **94** 083003

[11] Chelkowski S, Bredtmann T and Bandrauk A D 2012 *Phys. Rev. A* **85** 033404

[12] Kraus P, Mignolet B, Baykusheva D, Rupenyan A, Horný L, Penka E, Grassi G, Tolstikhin O, Schneider J, Jensen F, Madsen L, Bandrauk A, Remacle F and Wörner H 2015 *Science* **350** 790

[13] He L, Zhang Q, Lan P, Cao W, Zhu X, Zhai C, Wang F, Shi W, Li M, Bian X, Lu P and Bandrauk A D 2018 *Nat. Commun.* **9** 1108

[14] Li L, Lan P, He L, Cao W, Zhang Q and Lu P 2020 *Phys. Rev. Lett.* **124** 157403

[15] Goulielmakis E, Loh Z, Wirth A, Santra R, Rohringer N, Yakovlev V S, Zherebtsov S, Pfeifer T, Azzeer A M, Kling M F, Leone S R and Krausz F 2010 *Nature* **466** 739

[16] Ott C, Kaldun A, Argenti L, Raith P, Meyer K, Laux M, Zhang Y, Blättermann A, Hagstotz S, Ding T, Heck R, Madroñero J, Martín F and Pfeifer T 2014 *Nature* **516** 374

[17] Ossiander M, Siegrist F, Shirvanyan V, Pazourek R, Sommer A, Latka T, Guggenmos A, Nagele S, Feist J, Burgdörfer J, Kienberger R and Schultze M 2017 *Nat. Phys.* **13** 280

[18] Mauritsson J, Remetter T, Swoboda M, Klünder K, L'Huillier A, Schafer K J, Ghafur O, Kelkensberg F, Siu W, Johnsson P, Vrakking M J J, Znakovskaya I, Uphues T, Zherebtsov S, Kling M F, Lépine F, Benedetti E, Ferrari F, Sansone G and Nisoli M 2010 *Phys. Rev. Lett.* **105** 053001

[19] Klünder K, Johnsson P, Swoboda M, L'Huillier A, Sansone G, Nisoli M, Vrakking M J J, Schafer K J and Mauritsson J 2013 *Phys. Rev. A* **88** 033404

[20] Xu M, Peng L, Zhang Z and Gong Q 2011 *J. Phys. B: At. Mol. Opt. Phys.* **44** 021001

[21] Dixita G, Vendrella O and Santra R 2012 *Proc. Natl. Acad. Sci. USA* **109** 11636

[22] Shao H and Starace A 2010 *Phys. Rev. Lett.* **105** 263201

[23] Wörner H J and Corkum P B 2011 *J. Phys. B: At. Mol. Opt. Phys.* **44** 041001

[24] Fechner L, Camus N, Ullrich J, Pfeifer T and Moshammer R 2014 *Phys. Rev. Lett.* **112** 213001

[25] Yudin G L, Chelkowski S, Itatani J, Bandrauk A D and Corkum P B 2005 *Phys. Rev. A* **72** 051401

[26] Yuan K, Shu C, Dong D and Bandrauk A D 2017 *J. Phys. Chem. Lett.* **8** 2229

[27] Yuan K and Bandrauk A D 2017 *Phys. Chem. Chem. Phys.* **19** 25846

[28] Walt S, Ram N, Atala M, Shvetsov-Shilovski N, von Conta A, Baykusheva D, Lein M and Wörner H 2017 *Nat. Commun.* **8** 15651

[29] He M, Li Y, Zhou Y, Li M, Cao W and Lu P 2018 *Phys. Rev. Lett.* **120** 133204

[30] Haertelt M, Bian X, Spanner M, Staudte A and Corkum P B 2016 *Phys. Rev. Lett.* **116** 133001

[31] Huismans Y, Rouzée A, Gijsbertsen A, Jungmann J, Smolkowska A, Logman P, Lépine F, Cauchy C, Zamith S, Marchenko T, Bakker J, Berden G, Redlich B, Van der Meer A, Muller H, Vermin W, Schafer K, Spanner M, Ivanov M, Smirnova O, Bauer D, Popruzhenko S and Vrakking M 2011 *Science* **331** 61

[32] Liu M, Li M, Wu C, Gong Q, Staudte A and Liu Y 2016 *Phys. Rev. Lett.* **116** 163004
[33] Tan J, Zhou Y, Ke Q, He M, Liang J, Li Y, Li M and Lu P 2020 *Phys. Rev. A* **101** 013407
[34] Zhou Y, Tan J, Li M and Lu P 2021 *Sci. Chin.-Phys. Mech. Astron.* **64** 273011
[35] Zhou Y, Tolstikhin O I and Morishita T 2016 *Phys. Rev. Lett.* **116** 173001
[36] He M, Zhou Y, Li Y, Li M and Lu P 2017 *Opt. Quantum Electron.* **49** 232
[37] Tong X, Watahiki S, Hino K and Toshima N 2007 *Phys. Rev. Lett.* **99** 093001
[38] Despré V, Golubev N and Kuleff A 2018 *Phys. Rev. Lett.* **121** 203002
[39] Lara-Astiaso M, Ayuso D, Tavernelli I, Decleva P, Palacios A and Martin F 2016 *Faraday Discuss* **194** 41
[40] Arbó D G, Ishikawa K L, Schiessl K, Persson E and Burgdörfer J 2010 *Phys. Rev. A* **81** 021403
[41] Lindner F, Schätzel M G, Walther H, Baltuška A, Goulielmakis E, Krausz F, Milošević D B, Bauer D, Becker W and Paulus G G 2005 *Phys. Rev. Lett.* **95** 040401
[42] Arbó D G, Persson E and Burgdörfer J 2006 *Phys. Rev. A* **74** 063407
[43] Tolstikhin O I and Morishita T 2012 *Phys. Rev. A* **86** 043417
[44] Bian X and Bandrauk A D 2012 *Phys. Rev. Lett.* **108** 263003